Princeton Plasma Physics Laboratory

PPPL- 4336

PPPL- 4336

The Dimits Shift in More Realistic Gyrokinetic Plasma Turbulence Simulations

D.R. Mikkelsen and W. Dorland

July 2008

Prepared for the U.S. Department of Energy under Contract DE-AC02-76CH03073.

Princeton Plasma Physics Laboratory
Report Disclaimers

Full Legal Disclaimer

Trademark Disclaimer

PPPL Report Availability

Princeton Plasma Physics Laboratory:

http://www.pppl.gov/techreports.cfm

Office of Scientific and Technical Information (OSTI):

http://www.osti.gov/bridge

Related Links:

U.S. Department of Energy

Office of Scientific and Technical Information

Fusion Links

The Dimits Shift in More Realistic Gyrokinetic Plasma Turbulence Simulations

D. R. Mikkelsen*

Princeton Plasma Physics Laboratory,

P.O. Box 451, Princeton, NJ 08543

W. Dorland

University of Maryland, College Park, MD 20742

(Dated: Draft on July 21, 2008)

Abstract

In simulations of turbulent plasma transport due to long wavelength, ($k_\perp \rho_\mathrm{i} \leq 1$), electrostatic drift-type instabilities we find that a nonlinear upshift of the effective threshold persists. This 'Dimits shift' represents the difference between the linear threshold, at the onset of instability, and the nonlinear threshold, where transport increases suddenly as the driving temperature gradient is increased. As the drive increases, the magnitudes of turbulent eddies and zonal flows grow until the zonal flows become *nonlinearly* unstable to 'tertiary' modes and their sheared flows no longer grow fast enough to strongly limit eddy size. The tertiary mode threshold sets the effective nonlinear threshold for the heat transport, and the Dimits shift arises when this occurs at a zonal flow magnitude greater than that needed to limit transport near the linear threshold. Next-generation tokamaks will likely benefit from the higher effective threshold for turbulent transport, and transport models should incorporate suitable corrections to linear thresholds. These gyrokinetic simulations are more realistic than previous reports of a Dimits shift because they include nonadiabatic electron dynamics, strong collisional damping of zonal flows, and finite electron and ion collisionality together with realistic shaped magnetic geometry. Reversing previously reported results based on idealized adiabatic electrons, we find that increasing collisionality reduces the heat flux because collisionality reduces the nonadiabatic electron drive.

PACS numbers: 52.65.Tt, 52.25.Fi, 52.35.Qz, 52.55.Fa

*Electronic address: mikk@pppl.gov

Strongly correlated core and edge temperatures are commonly observed in current experiments (see section 3.2.5 of Ref. [1]) and in transport predictions for reactor-scale tokamaks [1, 2]. This is a consequence of transport 'stiffness', and is a feature of most theoretical models of turbulent plasma transport (see section 2.1.1 of Ref. [1]). Stiffness describes the rapidly increasing plasma heat flux as the appropriately normalized temperature gradient parameter, $R/L_{\rm T} \equiv -(R/T)(dT/dr)$, exceeds the threshold for microinstability. (Here, R is the major radius of the tokamak, and r is an appropriately chosen minor radius coordinate.) The practically achievable $R/L_{\rm T}$ is therefore only slightly larger than the threshold value [3], and the core temperature profile shape is close to the 'critical' profile found by integrating the normalized threshold temperature gradient, denoted by $R/L_{\rm T}^*(r)$, inwards from a boundary temperature in the plasma periphery. Since the temperature gradient scale length involves a logarithmic derivative, the *ratio* of the core and boundary temperatures is determined by $R/L_{\rm T}^*(r)$.

Achieving high fusion power multiplication is thus dependent on achieving sufficiently high edge temperatures, which may be problematic in reactor-scale devices. However, pioneering gyrokinetic studies [4, 5] revealed that $R/L_{\rm T}^*$ could be *larger* than the threshold for linear instability, and this unexpected gift of nature relaxes the edge temperature requirement. Understanding the physical processes that give rise to this 'Dimits shift' has been a goal of many studies [6–14]. It is clear that in the Dimits shift region – where the driving gradient is just above the threshold for linear stability – *nonlinear* effects reduce the turbulent transport to negligible levels. (Note that we differ from Ref. [9] by not using "Dimits shift" to denote *complete* quenching of turbulence.) Theoretical studies indicate that fast secondary instabilities [6–8, 15] drive zonal flows [9, 10, 13] which in turn greatly reduce the steady state transport [4, 16, 17]. These flows limit the turbulent eddy size and reduce the phase between the fluctuating potential and temperature. The effective threshold, $R/L_{\rm T}^*$, is defined by a rapid increase in transport fluxes that occurs only when the driven zonal flows grow sufficiently strong to excite tertiary instabilities that limit the strength of the zonal flows [6, 12], and thus allow the increased drive by larger $R/L_{\rm T}$ to raise the turbulent flux.

Although the existence of zonal flows driven by plasma turbulence was first noted long ago [18] and their major role in regulating simulated tokamak turbulence was established in 1993 [16], the complete quenching of turbulent transport by zonal flows was a surprise. This full suppression of transport [4] is understood to be a very special case that is "a consequence

of the approximation of zero or very low collisionality"[9], so the subject of this Letter is whether zonal flows can produce a strong suppression in more realistic simulations (we find they can).

Early on, it was recognized [4] that it is important to add collisions because they damp the otherwise persisitent zonal flows [19, 20] and to include nonadiabatic electron dynamics that strengthen the instability drive [21, 22]. In more complete simulations, the strengthened instabilities might overpower the viscously damped zonal flows and the upshift might be eliminated. The addition of collisions – with the continued neglect of nonadiabatic electron dynamics – *does* eliminate the complete quenching of turbulent transport in the Dimits shift regime [23, 24], and collisionality indirectly controls the transport by damping the zonal flows that in turn regulate the turbulence. Simulations with increased drive from nonadiabatic electron dynamics – but without collisional viscosity – demonstrated both increased transport [25] and a persistent Dimits shift [26].

Additional examples of a Dimits shift were observed in highly idealized simulations [27],D and in recent simulations with nonadiabatic electrons and shaped plasmas, both with collisions [28] and without [29]. Further examples of nonlinear upshift have been reported for turbulence driven by different instabilities – trapped electron modes [30], and resistive drift wave turbulence [31] – and in a stellarator [32]. The Dimits shift vanishes in a few situations [6, 27, 29, 33], but these seem to be exceptions (the tokamak cases are highly idealized, in any case).

We show here that the Dimits shift is a robust feature seen in more complete simulations of microturbulence that include collisional damping of zonal flows, nonadiabatic electron dynamics, realistic plasma geometry, multiple ion species, and reactor-relevant T_e/T_i and R/L_{ne}. Only subsets of these features have been included simultaneously in previous simulations.

The plasma parameters used are typical of ICRF heated EDA H-mode plasmas in Alcator C-Mod [34, 35]. These are similar to 'standard' ITER H-mode conditions [1] in several respects: flat density profiles, low impurity concentrations, and well equilibrated ion and electron temperatures. However, the collisionality is much higher than in ITER and in the studies cited above, so it is well suited to a test of whether the Dimits shift can be eliminated by strong collisional damping of zonal flows.

A detailed description of the discharge, including profile data, is available online in the

ITER Profile Database [1, 36] (shot 960116027). The major parameters are the plasma current $I_{\rm p}$=1.0 MA, major radius $R_{\rm o}$=0.67 m, vacuum magnetic field (at $R_{\rm o}$) $B_{\rm o}$=5.2 T, line-average electron density $\overline{n}_{\rm e}$=3.5 $10^{20}{\rm m}^{-3}$, and effective charge $Z_{\rm eff}$=1.5. The simulations are located at $r = 0.56a$, with $r/R_{\rm o}$=0.179, $T_{\rm e}$=$T_{\rm i}$=1.5 keV. The ion temperature profile has recently been measured [37] in C-Mod plasmas very similar to the one simulated here. As expected, due to strong temperature equilibration, the ion and electron temperature profiles are nearly equal – as assumed in the simulations. The fixed magnetic configuration is derived from a TRANSP calculation of the magnetohydrodynamic equilibrium, and the surface at $r = 0.56a$ is characterized by $q = 1.3$, magnetic shear $\hat{s}$=1.16, elongation $\kappa = 1.28$, triangularity $\delta = 0.12$, and radial derivatives $\kappa' = 0.24$, $\delta' = 0.30$, and the derivative of the Shafranov shift, $\Delta' = -0.088$. The radial variable is the normalized midplane minor radius.

The results presented below were generated by GS2, a time-dependent, nonlinear gyrokinetic drift-wave turbulence simulation code [38, 39] based on flux-tube geometry [40]. It has been extensively benchmarked with the FULL code [38, 41, 42], the GYRO code [43–45], the GEM code [46, 47], and the GENE and PG3EQ codes [47].

The nonlinear electrostatic simulations described here include long-wavelength modes with ($k_\perp \rho_{\rm i} \leq 1$), and non-adiabatic treatments of both the ions and electrons, as well as appropriate Lorentz collision operators for each of the species. Most simulations include only two species, electrons and deuterium, with $Z_{\rm eff}$=1.0, but a few simulations also include boron, raising $Z_{\rm eff}$ to 1.5 or 2. Electromagnetic effects are not expected to be strong for these plasmas because the normalized pressure β does not approach the ideal-MHD ballooning limit.

We use an analytic Miller 'local equilibrium' [48] formulation of the magnetic geometry. Qualitatively similar results for the C-Mod plasma studied here have been obtained using an EFIT equilibrium [49]. Linear and nonlinear instability thresholds are essentially local notions since nonlocal effects make it difficult to define these concepts in global simulations. We note however that global simulations with the C-Mod and ITER ρ_* values are closely approximated by flux-tube simulations [44].

The simulation results reported here are based on a midplane computational domain with dimensions of $63\rho_{\rm i}$ and $70\rho_{\rm i}$ in the poloidal and radial directions, respectively. The 7 $k_\perp$ are spaced evenly in the range $0 \geq k_\perp \rho_{\rm i} \leq 0.60$ and the radial grid spacing is $\rho_{\rm i}/2$. When the maximum $k_\perp \rho_{\rm i}$ was increased from 0.6 to 1.0 by raising the number of poloidal modes to 12,

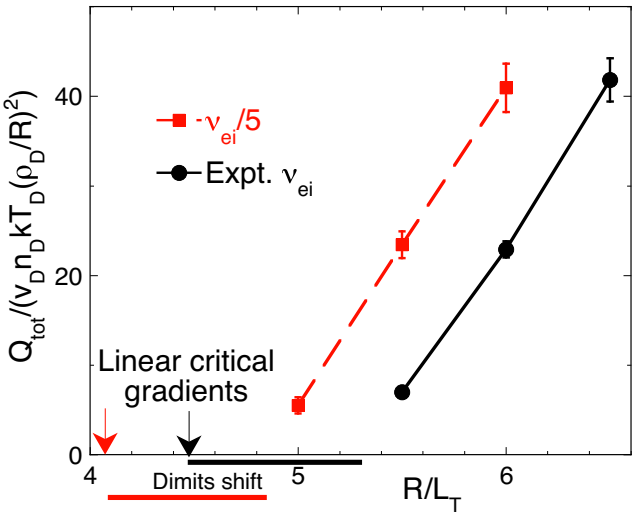

FIG. 1: The locations of both the linear and effective nonlinear thresholds depend on collisionality, but the size of the Dimits shift is not affected by collisionality. Transport is reduced by increasing collisionality because the nonadiabatic electron response is diminished, providing less 'amplification' of the ITG turbulence. $Q_{\rm tot}$ is the average transported power per unit area, $v_{\rm D} \equiv \sqrt{(T_{\rm D}/m_{\rm D})}$, $n_{\rm D}$, $T_{\rm D}$, $\rho_{\rm D}$, denote the deuterium thermal speed, density, temperature, and gyro-radius.

while slightly increasing the poloidal extent, the heat flux rose 22%.

Resolution and convergence will be fully discussed elsewhere. Based on a number of runs with varying maximum values of $k_\perp \rho_{\rm i}$, we expect that none of the results shown here would change significantly if modes up to $k_\perp \rho_{\rm i} = 1$ were included in the cases where this has not already been done in the convergence studies. Computational expense has prevented simulations that include even shorter wavelength modes, but these are not expected to qualitatively change the results because the turbulence has an ITG character [50, 51].

The total normalized heat flux from GS2 simulations is shown in Fig. 1, where both temperature gradient scale lengths are varied together for two series of simulations: one with the collisionality of the experimental conditions, and the other with a five-fold reduction (for both species) to approach the values typically found in other current-day tokamaks. The heat fluxes are 'offset linear', and the projected intercept at zero power is called the *effective nonlinear* threshold. The linear threshold is shown with arrows and the difference between the nonlinear and linear thresholds is known as the Dimits shift. As expected, lowering the collisionality strongly increases the nonadiabatic electron response – and, hence, the

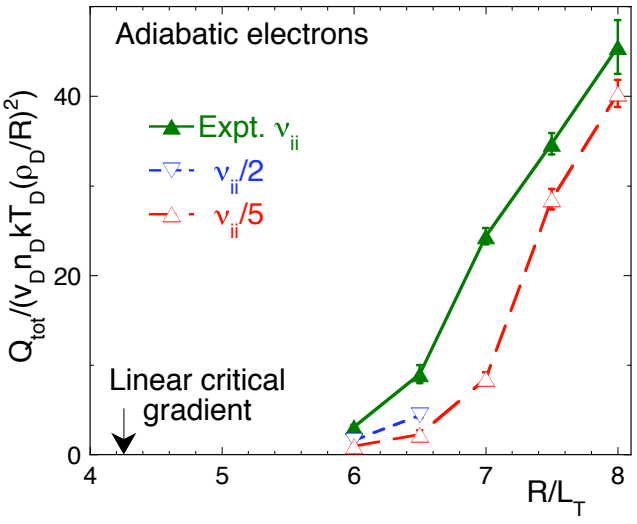

FIG. 2: Transport fluxes increase with collisionality when an adabatic electron model is used.

transport – thereby reducing the effective nonlinear threshold. Note that the linear stability threshold also moves, and thus a Dimits shift is observed in this case as well (contrary to the incorrect claim in Ref. [52], which assumed no change in the linear threshold).

The unchanged Dimits shift may be explained by the 'tertiary mode' paradigm [6, 12]: the nonlinear threshold occurs when the growing zonal flows reach the threshold for nonlinear 'tertiary' instabilities that subsequently prevent zonal flow growth, essentially placing a cap on the strength of the ExB shearing caused by the zonal flows. With lower collisionality the linear threshold is lower, so the turbulence and the zonal flow amplitudes begin to grow at lower driving gradients and the tertiary threshold is also attained at a lower driving gradient than required with higher collisionality.

The error bars shown for the heat fluxes are the "standard deviation of the mean" calculated from independent time-averages over many sub-intervals. The error bars are robustly independent of the sub-interval length *provided* it exceeds the typical eddy lifetime. Details will be given elsewhere; the method is available with the `vugyro` post-processor [43], and the GKV tools [53].

Lower collisionality was previously reported to *reduce* transport [23, 24], but only the effect of ion collisionality was included because the electron model was adiabatic [54, 55]. Here, as collisionality is decreased from its initially high level, the *nonadiabatic* electron amplification of the turbulence is strongly enhanced. This is evidently more important

than the weakened collisional damping of zonal flows that was central to the results in Ref. [23, 24].

The earlier result with adiabatic electrons is qualitatively confirmed in Fig. 2, where we also observe reduced heat transport *within the Dimits shift region* as the ion collisionality is lowered. With increasing temerature gradient drive, however, the zonal flows begin to excite tertiary modes [6] that become more important than collisional damping of zonal flows in the experimentaly relevant regime beyond the nonlinear threshold. This varying importance of collisional damping is closely parallel to that reported for turbulence driven by entropy modes in a Z-pinch [12]. Note also that the Dimits shift has grown, relative to Fig. 1, to become roughly as large as in the initial report [4]. This may be a consequence of the relatively sluggish increase in the growth rate in Fig. 4 (due to the absence of nonadiabatic electron amplification): a larger increase in driving gradient may be required to push the turbulently driven zonal flows to the threshold for tertiary instability that is presumed to cause the nonlinear threshold in Fig. 2. Two new qualitative results are apparent for the conditions of these simulations: the stiffness has a weak dependence on collisionality, as does the nonlinear threshold. The linear threshold is unchanged, so the Dimits shift is nearly independent of collisionality.

The adiabatic electron model is quite popular because it greatly reduces the computational cost, but the results are unreliable: the nonlinear threshold, the size of the Dimits shift, and the collisionality dependence all differ from more complete simulations that include nonadiabatic electron kinetics.

A moderately peaked density profile was inferred from limited measurements available at the time the C-Mod data was submitted to the ITER Profile Database, so our initial turbulence simulations used the reported $R/L_{\rm ne} = 1.2$. Additional diagnostics have subsequently revealed that this type of plasma actually has a very flat density profile [56, 57], so results from further simulations using $R/L_{\rm ne} = 0.1$ are shown in Fig. 3. We also included boron sufficient to raise $Z_{\rm eff}$ to 1.5 and 2.0 (Fig. 3). The linear thresholds are again indicated with arrows, and the Dimits shift is evident in all cases. Note that raising $Z_{\rm eff}$ above 1 increases the nonlinear threshold, but the Dimits shift is little changed (extrapolation from Q¿10 is used for $Z_{\rm eff} = 1$). Runs not shown indicate that the higher electron collisionality is not responsible for the shift, reduced deuterium density is the cause.

Recently, low-collisionality peaked-density H-modes have been produced in Alcator C-

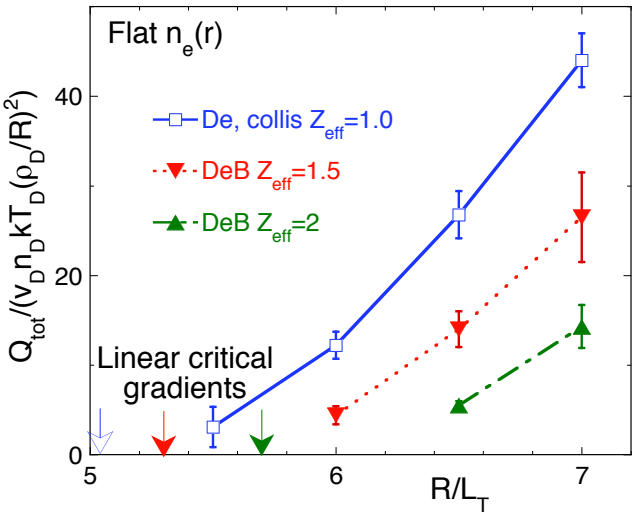

FIG. 3: Adding impurities shifts the linear and nonlinear thresholds (but not the Dimits shift). Three-species simulations, 'DeB', include kinetic treatment of deuterium, electrons and boron.

Mod [57], so both the peaked and flat-density simulations correspond to realizable C-Mod discharges, and both types are also considered plausible in large devices such as ITER [57].

A possible cause of the varying stiffness might be found in the dependence of the linear growth rates on R/L_T, shown in Fig. 4. There is a good match between the ordering of the slopes in Fig. 4 and the corresponding stiffness in Figs. 1 and 3, but this does not also hold for the adiabatic electron simulations. These have the least slope for the growth rates, but not the smallest stiffness. Perhaps changes in zonal flow tertiary stability play an important role in these cases.

A Dimits shift occurs in all of our realistic simulations of tokamak plasma turbulence that include collisional effects, gyrokinetic main ions, impurities and electrons, in realistic shaped tokamak geometry with parameters characteristic of present and future tokamak experiments. Previous work that found a reduction in transport as the collisionality was reduced [23, 24] is now overturned because the collisionality dependence of (previously ignored) nonadiabatic electron dynamics is more important than the collisional damping of zonal flows. However, the robust nature of the Dimits shift itself is an encouraging result for magnetic confinement fusion reactors.

It is a pleasure to thank G. W. Hammett, S. Scott, and R. E. Waltz for enlightening discussions. Extensive use of the parallel computers at the National Energy Research Sci-

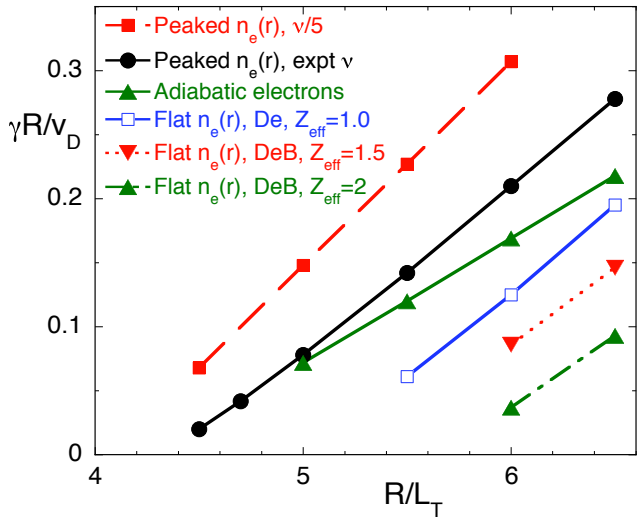

FIG. 4: Normalized growth rates for the fastest growing modes in each of the conditions shown in Figs. 1-3.

entific Computing Center (NERSC) and PPPL is gratefully acknowledged. This work was supported by U.S. Department of Energy Contract Nos. DE-AC02-76CH03073, DE-FG03-95ER54296 and DE-FC02-04ER54784.

---

[1] E. J. Doyle et al., Nucl. Fusion **47**, S18 (2007).

[2] ITER Physics Expert Groups on Confinement and Transport and Confinement Modelling and Database, ITER Physics Basis Editors and ITER EDA, Nucl. Fusion **39**, 2175 (1999).

[3] M. Kotschenreuther, W. Dorland, M. A. Beer, and G. W. Hammett, Phys. Plasmas **2**, 2381 (1995).

[4] A. M. Dimits et al., Phys. Plasmas **7**, 969 (2000).

[5] A. M. Dimits et al., in *Proc. 17th IAEA Fusion Energy Conf., Yokohama, 2000* (IAEA, Vienna, 1998), paper IAEA-CN-89/TH1/1.

[6] B. N. Rogers, W. Dorland, and M. Kotschenreuther, Phys. Rev. Lett. **85**, 5336 (2000).

[7] F. Jenko and W. Dorland, Phys. Rev. Lett. **89**, 225001 (2002).

[8] G. Plunk, Phys. Plasmas **14**, 112308 (2007).

[9] P. H. Diamond, S. Itoh, K. Itoh, and T. S. Hahm, Plasma Phys. & Controlled Fusion **47**, R35 (2005).

[10] R. A. Kolesnikov and J. A. Krommes, Phys. Plasmas **12**, 122302 (2005).

[11] Y. Idomura, T.-H. Watanabe, and H. Sugama, C. R. Physique **7**, 650 (2006).

[12] P. Ricci, B. N. Rogers, and W. Dorland, Phys. Rev. Lett. **97**, 245001 (2006).

[13] A. M. Dimits, W. M. Nevins, D. E. Shumaker, G. W. Hammett, T. Dannert, et al., Nucl. Fusion **47**, 817 (2007).

[14] T.-H. Watanabe, H. Sugama, and S. Ferrando-Margalet, Nucl. Fusion **47**, 1383 (2007).

[15] S. C. Cowley, R. M. Kulsrud, and R. Sudan, Phys. Fluids B **3**, 2767 (1991).

[16] G. W. Hammett, M. A. Beer, W. Dorland, S. C. Cowley, and S. A. Smith, Plasma Phys. & Controlled Fusion **35**, 973 (1993).

[17] Z. Lin, T. S. Hahm, W. W. Lee, W. M. Tang, and R. B. White, Science **281**, 1835 (1998).

[18] A. Hasegawa and M. Wakatani, Phys. Rev. Lett. **59**, 1581 (1987).

[19] F. L. Hinton and M. N. Rosenbluth, Plasma Phys. & Controlled Fusion **41**, A653 (1999).

[20] H. Sugama and T.-H. Watanabe, Phys. Rev. Lett. **94**, 115001 (2005).

[21] G. Rewoldt and W. M. Tang, Phys. Fluids B: Plasma Phys. **2**, 318 (1990).

[22] F. Romanelli and S. Briguglio, Phys. Fluids B: Plasma Phys. **2**, 754 (1990).

[23] Z. Lin, T. S. Hahm, W. W. Lee, W. M. Tang, and P. H. Diamond, Phys. Rev. Lett. **83**, 3645 (1999).

[24] Z. Lin, T. S. Hahm, W. W. Lee, W. M. Tang, and R. B. White, Phys. Plasmas **7**, 1857 (2000).

[25] Y. Chen and S. Parker, Phys. Plasmas **8**, 2095 (2001).

[26] S. E. Parker, Y. Chen, W. Wan, B. I. Cohen, and W. M. Nevins, Phys. Plasmas **11**, 2594 (2004).

[27] A. M. Dimits, B. I. Cohen, W. M. Nevins, and D. E. Shumaker, Nucl. Fusion **41**, 1725 (2001).

[28] E. A. Belli, Ph.D. thesis, Princeton University, Princeton, NJ 08544 (2006).

[29] J. E. Kinsey, R. Waltz, and J. Candy, Phys. Plasmas **14**, 102306 (2007).

[30] D. R. Ernst, P. T. Bonoli, P. J. Catto, W. Dorland, C. L. Fiore, R. S. Granetz, M. Greenwald, A. E. Hubbard, M. Porkolab, M. H. Redi, et al., Phys. Plasmas **11**, 2637 (2004).

[31] R. Numata, R. Ball, and R. L. Dewar, Phys. Plasmas **14**, 102312 (2007).

[32] P. Xanthopoulos, F. Merz, T. Görler, and F. Jenko, Phys. Rev. Lett. **99**, 035002 (2007).

[33] F. Merz et al., Bull. Amer. Phys. Soc. **52**, 277 (2007), TO3.00002.

[34] Y. Takese et al., Phys. Plasmas **4**, 1647 (1997).

[35] M. Greenwald et al., Nucl. Fusion **37**, 793 (1997).

[36] D. Boucher et al., Nucl. Fusion **40**, 1955 (2000).

[37] A. Ince-Cushman et al., Bull. Amer. Phys. Soc. **52**, 231 (2007), PO3.00014.

[38] M. Kotschenreuther, G. Rewoldt, and W. M. Tang, Comp. Phys. Comm. **88**, 128 (1995).

[39] W. Dorland, F. Jenko, M. Kotschenreuther, and B. N. Rogers, Phys. Rev. Lett. **85**, 5579 (2000).

[40] M. A. Beer, S. C. Cowley, and G. W. Hammett, Phys. Plasmas **2**, 2687 (1995).

[41] E. Belli, W. Dorland, G. W. Hammett, and M. C. Zarnstorff, Bull. Amer. Phys. Soc. **46**, 232 (2001).

[42] C. Bourdelle et al., Phys. Plasmas **10**, 2881 (2003).

[43] J. Candy and R. Waltz, J. Comp. Phys. **186**, 545 (2003).

[44] J. Candy, R. Waltz, and W. Dorland, Phys. Plasmas **11**, L25 (2004).

[45] W. M. Nevins et al., Phys. Plasmas **13**, 122306 (2006).

[46] Y. Chen et al., Nucl. Fusion **43**, 1121 (2003).

[47] W. M. Nevins et al., Phys. Plasmas **14**, 084501 (2007).

[48] R. L. Miller et al., Phys. Plasmas **5**, 973 (1998).

[49] D. W. Ross, Univ. of Texas (2001), private communication.

[50] R. Waltz, J. Candy, and M. Fahey, Phys. Plasmas **14**, 056116 (2007).

[51] J. Candy, R. Waltz, M. Fahey, and C. Holland, Plasma Phys. & Controlled Fusion **49**, 1209 (2007).

[52] D. R. Mikkelsen et al., in *Proc. 19th IAEA Fusion Energy Conf., Lyon, 2002* (IAEA, Vienna, 2002), paper IAEA-CN-94/EX/P5-03.

[53] W. M. Nevins, "GKV User's Manual" (unpublished).

[54] W. Dorland and G. W. Hammett, Phys. Fluids B **5**, 812 (1993).

[55] B. I. Cohen, T. J. Williams, A. M. Dimits, and J. A. Byers, Phys. Fluids B **5**, 2967 (1993).

[56] E. S. Marmar et al., Nucl. Fusion **43**, 1610 (2003).

[57] M. Greenwald et al., Nucl. Fusion **47**, L26 (1997).

The Princeton Plasma Physics Laboratory is operated
by Princeton University under contract
with the U.S. Department of Energy.

Information Services
Princeton Plasma Physics Laboratory
P.O. Box 451
Princeton, NJ 08543

Phone: 609-243-2750
Fax: 609-243-2751
e-mail: pppl_info@pppl.gov
Internet Address: http://www.pppl.gov